

Quark-gluon plasma phenomenology from the lattice

Chris Allton^{1,*}, Gert Aarts¹, Alessandro Amato^{1,2}, Wynne Evans^{1,3},
 Pietro Giudice^{1,4}, Simon Hands¹, Aoife Kelly⁵, Seyong Kim⁶,
 Maria-Paola Lombardo⁷, Sinead Ryan⁸, Jon-Ivar Skullerud⁵,
 Tim Harris⁸

¹ Department of Physics, College of Science, Swansea University, Swansea SA2 8PP, U.K.

² Institute for Theoretical Physics, Universität Regensburg, D-93040 Regensburg, Germany

³ Fakultät für Physik, Universität Bielefeld, D-33615 Bielefeld, Germany

⁴ Institut für Theoretische Physik, Universität Münster, Germany

⁵ Department of Mathematical Physics, NUIM, Maynooth, Co. Kildare, Ireland

⁶ Department of Physics, Sejong University, Seoul 143-747, Korea

⁷ INFN-Laboratori Nazionali di Frascati, I-00044, Frascati (RM) Italy

⁸ School of Mathematics, Trinity College, Dublin 2, Ireland

* Speaker

E-mail: c.allton@swan.ac.uk

Abstract.

The FASTSUM Collaboration has calculated several quantities relevant for QCD studies at non-zero temperature using the lattice technique. We report here our results for the (i) interquark potential in charmonium; (ii) bottomonium spectral functions; and (iii) electrical conductivity. All results were obtained with 2+1 flavours of dynamical fermions on an anisotropic lattice which allows greater resolution in the temporal direction.

1. Introduction

The Particle Data Book [1] is a repository of particle physics knowledge, and yet it contains no entries on the deconfined phase of QCD. We present here some lattice calculations of phenomena in the quark-gluon plasma (QGP) phase with the ultimate aim of addressing this omission.

The lattice approach is based on the non-perturbative study of correlation functions of operators calculated in a background of glue and dynamical (sea) quarks using the imaginary time (i.e. Euclidean) formulation¹. For instance, to study the η_c system, correlators, $C(\tau)$, of the operator $J = \bar{c}\gamma_5 c$ are determined (c is the charm quark field). Each state i which has the same quantum numbers as J (and therefore can be excited by it) contributes a term $\sim e^{-M_i\tau}$ to $C(\tau)$, where M_i is the mass of state i . For large τ , only the ground state remains, and its properties can be determined.

While the lattice technique has had many successes in calculating phenomenologically relevant quantities at zero chemical potential, μ , particularly in the confined phase of QCD, it has a significant limitation for $\mu > 0$. This is the well-known “sign problem” which has haunted efforts to extend our knowledge into the entire (T, μ) plane².

¹ For a general introduction to lattice gauge theory see [2], and non-zero temperature reviews, see [3, 4].

² For reviews of the sign problem, see [5].

In this talk, I will discuss three lattice results obtained by the FASTSUM Collaboration at $\mu = 0$ and non-zero temperature, T , above and below the deconfining temperature, T_c , all produced on our 2+1 flavour, anisotropic lattices. These topics are a calculation of the potential in the charmonium system (Sec.2), bottomonium spectral functions (Sec.3), and a determination of the electrical conductivity of QCD as a function of T (Sec.4).

This work uses lattice simulations with the parameters in Table 1 and a carefully crafted action with reduced lattice artefacts [6]. Anisotropic rather than isotropic lattices provide a distinct advantage due to the finer temporal resolution and correspondingly larger sampling of the correlator, $C(\tau)$. This is particularly significant in the $T > 0$ case where the temporal extent is limited to $0 \leq \tau \leq 1/T$. Our T_c value is obtained from the Polyakov Loop.

N_s	32	24	24	24	32	24	32	24	32	24	24	32
N_τ	48	40	36	32	32	28	28	24	24	20	16	16
$T(\text{MeV})$	117	141	156	176	176	201	201	235	235	281	352	352
T/T_c	0.63	0.76	0.84	0.95	0.95	1.09	1.09	1.27	1.27	1.52	1.90	1.90

Table 1. Lattice parameters used where $N_{(s)\tau}$ is the number of sites in the spatial (temporal) direction. Our spatial and temporal lattice spacings are $a_s = 0.1227(8)$ and $a_\tau = 0.0351(2)$ fm.

2. Charmonium potential

The interquark potential in charmonium is of great interest to phenomenologists modelling the QGP phase in heavy ion collisions. Knowledge of this potential aids our understanding of the J/ψ system, and the extent to which states become unbound with increasing temperature.

Lattice calculations of the finite temperature interquark potential have, until recently, been restricted to the static (i.e. infinitely heavy) quark limit [7]. On the other hand, the finite-mass interquark potential has been calculated at $T = 0$ [8] using the method developed by the HAL QCD collaboration for internucleon potentials [9]. This method first calculates the wavefunction of the two-particle system, $\psi(r)$, which is then used as input into the Schrödinger equation, yielding the potential, $V(r)$, as output.

In our case, we consider non-local operators of (charm) quark fields, $J(x, \mathbf{r}) = c(x)\Gamma U(x, x + \mathbf{r})\bar{c}(x + \mathbf{r})$, where Γ is an appropriately chosen Dirac (gamma) matrix, and $U(x, x + \mathbf{r})$ is the gauge connection between x and $x + \mathbf{r}$ [10]. The correlation function of these operators is

$$C(\mathbf{r}, \tau) = \sum_{\mathbf{x}} \langle J(x, \mathbf{r}) J^\dagger(x, \mathbf{0}) \rangle = \sum_i \frac{\psi_i(\mathbf{r}) \psi_i^*(\mathbf{0})}{2M_i} e^{-M_i \tau}, \quad (1)$$

where the second sum is over the states i . Following [11], $C(\mathbf{r}, \tau)$ satisfies the Schrödinger equation which can then be used to extract the potential.

As usual, the potential can be decomposed into the central, $V_C(r)$, and the spin dependent, $V_S(r)$, terms, $V_\Gamma(r) = V_C(r) + \mathbf{s}_1 \cdot \mathbf{s}_2 V_S(r)$, where $\mathbf{s}_{1,2}$ are the spins of the charm quarks. In Fig.1 (Left), we show the charmonium central potential, $V_C(r)$ thus obtained at various temperatures above and below the deconfining temperature. We use $N_s = 24$ in this work. Also shown is another determination of this potential, but obtained in the static quark limit [12]. As can be seen, there is a clear temperature dependence in our calculated potential which becomes less confining as T increases. In Fig.1 (Right) $V_S(r)$, is plotted showing a repulsive core with a temperature variation at large distances.

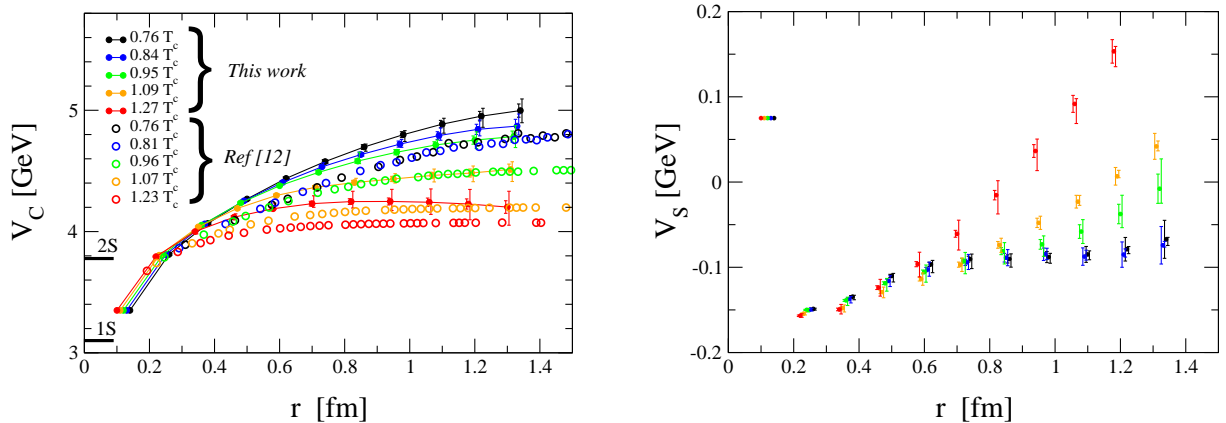


Figure 1. (Left) The charmonium central potential, $V_C(r)$, together with the results from a static quark calculation [12]. (Right) The charmonium spin dependent potential, $V_S(r)$.

3. Bottomonium spectral functions

In this section we discuss our studies of bottomonium at $T > 0$. Recent results from CMS show that the 1S and 2S/3S Υ states have different relative multiplicities in Pb-Pb compared to p-p collisions at the LHC [13]. This result confirms the picture, originally proposed in the charmonium system, in which the higher mass states in quarkonium are the first to become unbound as the temperature increases beyond T_c [14].

We have performed lattice simulations of the bottomonium system using an $\mathcal{O}(v^4)$ NRQCD lattice action [15] to represent the b -quarks. This extends our earlier work [16]. NRQCD is an approximation obtained from QCD as a velocity expansion in v/c , and is thus applicable for b -quarks. The advantages of NRQCD over the (exact) relativistic quark formulation are two-fold. There is no periodicity in time which complicates the correlation function: in the relativistic case, backward movers effectively half the number of time points that carry independent information. The lack of these thermal boundary effects means that the NRQCD quarks should be viewed as test colour charges moving in a thermal bath of dynamical light quarks and gluons. Secondly, the solution of the NRQCD propagator is an initial value problem which is much easier to solve than the matrix inversion required in the relativistic case. Thus, for a given computer resource, much higher statistics can be achieved in the NRQCD case.

The spectral function, $\rho(\omega)$, can be defined from the two-point correlation function, $C(\tau)$, of bottomonium operators via

$$C(\tau) = \int \rho(\omega) K(\tau, \omega) d\omega, \quad (2)$$

where in the NRQCD case the kernel is $K(\tau, \omega) = \exp(-\omega\tau)$. In principle, the spectral function contains complete information on the states in the channel considered. For a stable particle of mass M , $\rho(\omega) \propto \delta(\omega - M)$. For a resonance, this δ -function broadens acquiring a non-zero width, and if the state becomes unbound, the spectral feature disappears.

We have used the Maximum Entropy Method (MEM), a Bayesian technique, to de-convolve eq.(2) to extract $\rho(\omega)$ [17]. The results for the S -wave (Υ) channel and P -wave (χ_{b1}) channels are shown in Fig.2, all obtained with $N_s = 24$. There is a distinct temperature dependence in both channels. While the Υ ground state (1S) peak is seen to decrease with T , it remains a distinct (i.e. bound) feature up to $T \approx 1.90T_c$. However, the excited state (2S) peak seems to disappear for $T \gtrsim T_c$. This agrees with the experimental result obtained by the CMS collaboration [13]. These results contrast with the χ_{b1} case where the ground state (1P) appears to melt at $T \approx T_c$, see Fig.2 (Right).

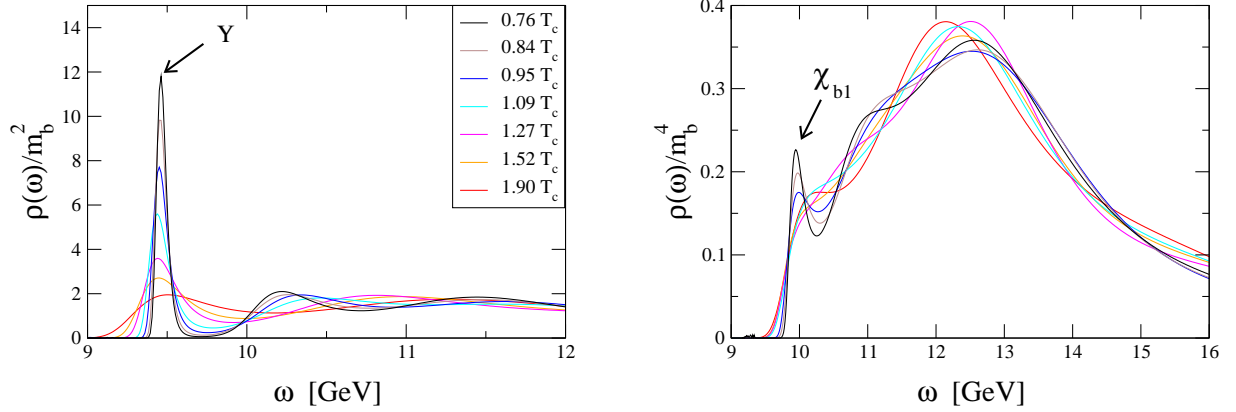


Figure 2. The NRQCD Bottomonium S -wave (Left) and P -wave (Right) spectral functions.

4. Electrical conductivity

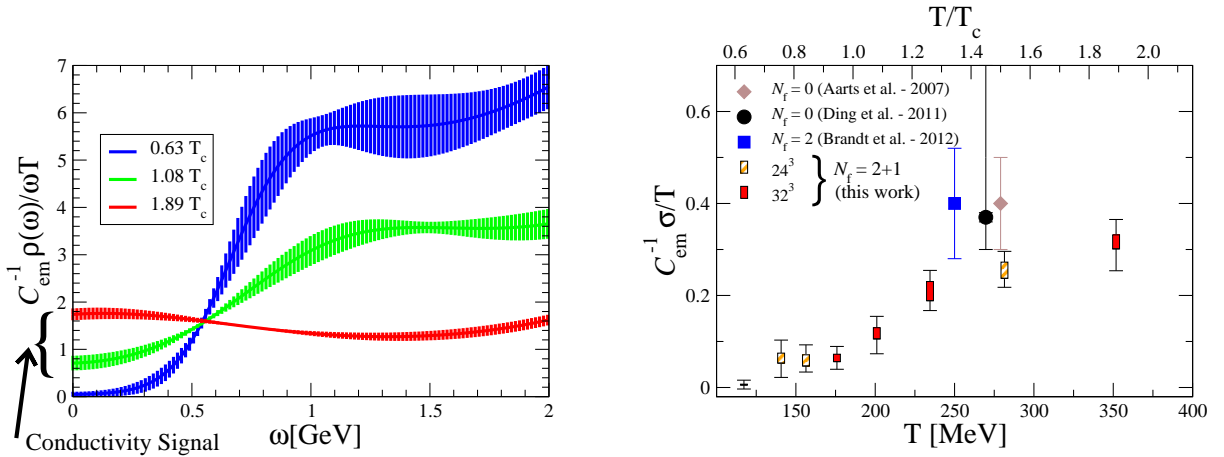


Figure 3. The (light-quark) electromagnetic spectral function, $\rho^{\text{em}}(\omega)$, showing the conductivity signal in the $\omega \rightarrow 0$ limit. $C_{\text{em}} = 5/9e^2$ for two light flavours.

Figure 4. The conductivity, σ , as a function of temperature. As well as the results from our work, quenched ($N_f = 0$) [19, 20] and dynamical results [21] are also shown.

We now discuss our calculation of the electrical conductivity, σ [18]. Transport coefficients such as σ are of special relevance for understanding the bulk properties of the fireball in relativistic heavy-ion collision experiments. Typically, they can be determined from the zero energy limit of the appropriate spectral function, i.e. $\lim_{\omega \rightarrow 0} \rho/\omega$. In the case of the conductivity, the correlator to consider is that of the electromagnetic current of quark flavour f ,

$$C^{\text{em}}(\tau) = \sum_i \int d^3x \langle j_i^{\text{em}}(\tau, \mathbf{x}) j_i^{\text{em}}(0, \mathbf{x})^\dagger \rangle \quad \text{with} \quad j_i^{\text{em}}(x) = e \sum_f q_f j_i^f(x), \quad (3)$$

where e is the electron's charge, $q_f = \frac{2}{3}, -\frac{1}{3}$, is the fractional charge and $j_i^f \sim \bar{\psi}^f \gamma_i \psi^f$ the number density current of quark field ψ^f . In our case [18] we use the conserved lattice vector current (i.e. $\partial_\mu j_\mu^f = 0$) which means we do not have to renormalise our results. We again use MEM to invert the correlator to extract the corresponding $\rho^{\text{em}}(\omega)$, see Eq(2), but this time with the relativistic kernel $K(\tau, \omega) = \cosh[\omega(\tau - 1/2T)]/\sinh[\omega/2T]$.

The conductivity is obtained via the Kubo relation,

$$\frac{\sigma}{T} = \frac{1}{6T} \lim_{\omega \rightarrow 0} \frac{\rho^{\text{em}}(\omega)}{\omega}. \quad (4)$$

Fig.3 shows $\rho^{\text{em}}(\omega)$ around $\omega \approx 0$ for three temperatures spanning T_c . There is a clear non-zero intercept at $\omega = 0$ for $T \gtrsim T_c$, indicating a conductivity signal. In Fig.4, we present our σ values for all the T values we studied. The dimensionless ratio σ/T increases across the transition temperature. Results from three other published works are also shown [19, 20, 21].

5. Conclusion

In this talk, I have summarised our collaboration's lattice calculations showing that the charmonium potential becomes less binding with higher T , that the $\Upsilon(1S)$ state survives above T_c but the $\Upsilon(2S)$ and χ_{b1} don't, and that the conductivity increases with T across the transition.

References

- [1] J. Beringer *et al.* [Particle Data Group Collaboration], Phys. Rev. D **86** (2012) 010001.
- [2] I. Montvay, G. Münster, "Quantum Fields on a Lattice", Cambridge Monographs on Mathematical Physics.
- [3] L. Levkova, PoS LATTICE **2011** (2011) 011 [arXiv:1201.1516 [hep-lat]].
- [4] M. P. Lombardo, PoS LATTICE **2012** (2012) 016 [arXiv:1301.7324 [hep-lat]].
- [5] P. de Forcrand, PoS LAT **2009** (2009) 010 [arXiv:1005.0539 [hep-lat]]. G. Aarts, PoS LATTICE **2012** (2012) 017 [arXiv:1302.3028 [hep-lat]].
- [6] R. G. Edwards, B. Joo and H. -W. Lin, Phys. Rev. D **78** (2008) 054501 [arXiv:0803.3960 [hep-lat]].
- [7] O. Kaczmarek, F. Karsch, F. Zantow and P. Petreczky, Phys. Rev. D **70**, 074505 (2004) [Erratum-ibid. D **72**, 059903 (2005)] [hep-lat/0406036], Y. Maezawa *et al.* [WHOT-QCD Collaboration], Phys. Rev. D **75**, 074501 (2007) [hep-lat/0702004], A. Mócsy and P. Petreczky, Phys. Rev. D **77**, 014501 (2008) [arXiv:0705.2559 [hep-ph]], Z. Fodor, A. Jakóvác, S. D. Katz and K. K. Szabo, PoS LAT **2007**, 196 (2007) [arXiv:0710.4119 [hep-lat]], P. Petreczky, C. Miao and A. Mócsy, Nucl. Phys. A **855**, 125 (2011) [arXiv:1012.4433 [hep-ph]]. A. Bazavov and P. Petreczky, [arXiv:1210.6314 [hep-lat]]. Y. Burnier and A. Rothkopf, Phys. Rev. D **86**, 051503 (2012) [arXiv:1208.1899 [hep-ph]].
- [8] Y. Ikeda and H. Iida, PoS LATTICE **2010**, 143 (2010) [arXiv:1011.2866 [hep-lat]], T. Kawanai and S. Sasaki, Phys. Rev. Lett. **107**, 091601 (2011) [arXiv:1102.3246 [hep-lat]], Phys. Rev. D **85**, 091503 (2012) [arXiv:1110.0888 [hep-lat]], PoS LATTICE **2011**, 126 (2011) [arXiv:1111.0256 [hep-lat]], H. Iida and Y. Ikeda, PoS LATTICE **2011**, 195 (2011).
- [9] N. Ishii, S. Aoki and T. Hatsuda, Phys. Rev. Lett. **99**, 022001 (2007) [nucl-th/0611096], S. Aoki, T. Hatsuda and N. Ishii, Prog. Theor. Phys. **123**, 89 (2010) [arXiv:0909.5585 [hep-lat]], S. Aoki *et al.* [HAL QCD Collaboration], [arXiv:1206.5088 [hep-lat]]. N. Ishii [HAL QCD Collaboration], PoS LATTICE **2011**, 160 (2011), N. Ishii *et al.* [HAL QCD Collaboration], Phys. Lett. B **712** (2012) 437 [arXiv:1203.3642 [hep-lat]].
- [10] C. R. Allton, P. W. M. Evans and J. -I. Skullerud, PoS LATTICE **2012** (2012) 082 [arXiv:1306.3140 [hep-lat]]. P. W. M. Evans, C. R. Allton and J. -I. Skullerud, arXiv:1303.5331 [hep-lat]. P. W. M. Evans, C. Allton, P. Giudice and J. -I. Skullerud, PoS LATTICE **2013** (2013) 168 arXiv:1309.3415 [hep-lat].
- [11] N. Ishii [HAL QCD Collaboration], PoS LATTICE **2011**, 160 (2011), N. Ishii *et al.* [HAL QCD Collaboration], Phys. Lett. B **712** (2012) 437 [arXiv:1203.3642 [hep-lat]].
- [12] O. Kaczmarek and F. Zantow, Phys. Rev. D **71**, 114510 (2005) [hep-lat/0503017].
- [13] S. Chatrchyan *et al.* [CMS Collaboration], Phys. Rev. Lett. **107** (2011) 052302 [arXiv:1105.4894 [nucl-ex]].
- [14] T. Matsui and H. Satz, Phys. Lett. B **178**, 416 (1986).
- [15] G. T. Bodwin, E. Braaten and G. P. Lepage, Phys. Rev. D **51** (1995) 1125 [Erratum-ibid. D **55** (1997) 5853] [hep-ph/9407339].
- [16] G. Aarts, S. Kim, M. P. Lombardo, M. B. Oktay, S. M. Ryan, D. K. Sinclair and J. -I. Skullerud, Phys. Rev. Lett. **106** (2011) 061602 [arXiv:1010.3725 [hep-lat]], G. Aarts, C. Allton, S. Kim, M. P. Lombardo, M. B. Oktay, S. M. Ryan, D. K. Sinclair and J. I. Skullerud, JHEP **1111** (2011) 103 [arXiv:1109.4496 [hep-lat]], JHEP **1303** (2013) 084 [arXiv:1210.2903 [hep-lat]].
- [17] M. Asakawa, T. Hatsuda and Y. Nakahara, Prog. Part. Nucl. Phys. **46** (2001) 459 [hep-lat/0011040].
- [18] A. Amato, G. Aarts, C. Allton, P. Giudice, S. Hands and J. -I. Skullerud, arXiv:1307.6763 [hep-lat].
- [19] G. Aarts, C. Allton, J. Foley, S. Hands and S. Kim, Phys. Rev. Lett. **99** (2007) 022002.
- [20] H. -T. Ding *et al.*, Phys. Rev. D **83** (2011) 034504.
- [21] B. B. Brandt, A. Francis, H. B. Meyer and H. Wittig, JHEP **1303** (2013) 100.